Journal of Zhejiang University-SCIENCE A (Applied Physics & Engineering)
ISSN 1673-565X (Print); ISSN 1862-1775 (Online)
www.jzus.zju.edu.cn; www.springerlink.com
E-mail: jzus@zju.edu.cn

Nonlinear analysis of pile groups subjected to combined lateral and torsional loading*

Ling-gang KONG†, Zhong-chang ZHANG, Yun-min CHEN

Institute of Geotechnical Engineering, College of Architectural and Civil Engineering, Zhejiang University, Hangzhou 310058, China

†E-mail: klg@zju.edu.cn

Received Nov. 18, 2019; Revision accepted Feb. 12, 2020; Crosschecked Feb. 26, 2020

Abstract: An empirical approach has been developed to analyze the nonlinear response of a pile group with arbitrarily distributed piles subjected to combined lateral and torsional loading. In this approach, the concept of instantaneous twist center is applied to analyze the displacement relationship of pile heads and establish the static equilibrium equations of the pile cap. The horizontal interaction among the individual piles is considered through the generalized *p*-multiplier. The coupling effect of lateral resistance on the torsional resistance of each pile is quantified using an empirical factor β; the lateral and torsional nonlinear responses of individual piles are modeled by *p*-*y* and τ-θ curves, respectively. The proposed approach not only captures the most significant aspect of the group effect and coupling effect in a pile group subjected to combined lateral and torsional loading, but also automatically updates *p*-multipliers of individual piles based on pile cap displacements. The proposed approach was verified using results of model tests on pile groups subjected to lateral loading, torsional loading, and combined lateral and torsional loading, separately. In general, the pile cap response and the transfer of applied loads in the pile groups agree well with the test results.

Key words: Combined lateral and torsional loading; Pile groups; Twist center; *p*-multiplier; Group effect
https://doi.org/10.1631/jzus.A1900590 **CLC number:** TU413

1 Introduction

Research on single piles and pile groups subjected to torsion and combined lateral and torsional loading has received much attention in recent years (Hu et al., 2006; Kong and Zhang, 2007, 2008a, 2008b, 2009; He et al., 2010; Gu et al., 2014; Kong et al., 2015, 2019; Li, 2015; Chen et al., 2016; Li and Stuedlein, 2018; Mehra and Trivedi, 2018; Li et al., 2019). Hu et al. (2006), Kong and Zhang (2008b), Kong et al. (2015), and Li et al. (2019) investigated the response of single piles subjected to combined lateral and torsional loads and found the deflection-torsion coupling effect. Gu et al. (2014) and Kong et al. (2015) conducted model tests on pile groups under combined lateral and torsional loading and observed that: (1) the pile cap motion of a pile group is a combination of horizontal and torsional movements; (2) due to the twist of the pile cap, the pile head horizontal displacements as well as the mobilized pile head bending moments and shear forces in the piles differ significantly in both magnitude and direction; (3) the instantaneous center of the pile cap changes with the load eccentric distance. In addition, the group effect was considered to exist in a pile group subjected to combined lateral and torsional loading (Kong et al., 2015). The group effect of a pile group under torsional loading was significantly different from that under lateral loading (Kong and Zhang, 2008b).

* Project supported by the National Natural Science Foundation of China (Nos. 50809060 and 51579218) and the Fundamental Research Funds for the Central Universities, China (No. 2011QNA4013)
ORCID: Ling-gang KONG, https://orcid.org/0000-0002-5824-1275; Zhong-chang ZHANG, https://orcid.org/0000-0001-8172-2221

Kong and Zhang (2009) and Chen et al. (2016) theoretically discussed three types of interactions in torsionally loaded pile groups: the horizontal interaction between two identical piles subjected to horizontal loads in arbitrary directions, the torsional-horizontal interactions between two piles, and the interactions among the piles under torsion. Li (2015) further discussed the three types of interactions in pile groups subjected to combined lateral and torsional loading in theory and found that the first interaction had a dominant effect on the response of the pile groups. Kong et al. (2019) reported an experimental study on the horizontal interaction between two piles in a pile group subjected to combined lateral and torsional loading. First, they studied the characteristics of motions of two individual piles in a pile group under combined lateral and torsional loading, and then they performed centrifuge model tests, numerical analysis, and theoretical analysis to quantify the horizontal interaction between two piles using the concept of a reduction factor, as proposed by Reese et al. (2006). The reduction factor is defined as the ratio of the pile head horizontal resistance of one pile in a pile group to that of a single pile under the same displacement condition. It was found that the reduction factor varies with the angles between the directions of motion of the two piles and the line through both piles. Finally, multiplier factors were used by Kong et al. (2019) to quantify the dominant group effect in pile groups subjected to combined lateral and torsional loading. The multiplier factor of pile i in a pile group with n piles $f_{\mathrm{m}i}$ was calculated by

$$f_{\mathrm{m}i} = \beta_{1i}\beta_{2i}\cdots\beta_{ji}\cdots\beta_{ni}, \quad j \neq i, \tag{1}$$

where β_{ji} is the reduction factor of pile i due to the adjacent pile j. Eq. (1) was originally proposed by Reese et al. (2006) to calculate p-multipliers for pile groups subjected to lateral loading. The p-multiplier is a constant factor used to reduce a single-pile p-y curve to obtain a group-pile p-y curve, where p represents the lateral soil resistance per unit length of the pile and y is the lateral deflection of the pile (Brown et al., 1988). The approach proposed by Kong et al. (2019) also accurately predicts the multiplier factors for pile groups subjected to lateral loading and torsion. Therefore, their approach is herein referred to as the generalized p-multiplier approach.

Some numerical programs can predict the linear response of pile groups subjected to combined lateral and torsional loading (Randolph, 1980; Xu and Poulos, 2000; Li, 2015). Yet, approaches to predict the nonlinear response of pile groups subjected to such a loading have not been reported. A nonlinear model was proposed by He et al. (2010) to simulate the response of pile groups under torsion. In their model, p-y curve method is used to calculate the lateral resistance, and torsion rigidity theory is used to calculate the torsional resistance of the individual piles. However, the requirement for a centrosymmetric distribution of group piles and a lack of p-multipliers restrict the practical application of this approach. In this study, an approach is proposed to analyze the nonlinear response of a pile group with arbitrarily distributed piles subjected to combined lateral and torsional loads using the generalized p-multiplier. In this approach, the lateral resistance of the individual piles in a pile group is modeled by nonlinear p-y curves (Reese et al., 2006; Xue et al., 2016) and the torsional resistance by τ-θ curves (Kong, 2006; Li and Stuedlein, 2018), where τ is the torsional shear stress, and θ is the local twist angle of the pile shaft. The generalized p-multiplier is used to characterize interaction among lateral resistances of the individual piles, and a factor is used to take account of the deflection-torsion coupling effect in individual piles. Since the p-multipliers for individual piles vary with the direction of motion of the piles, an iteration scheme is developed to calculate the p-multiplier values and the pile head displacements of the piles. Approximate equilibrium equations of the pile cap are derived to improve the computational efficiency in iteration. A series of experimental results on pile groups under lateral loading, torsional loading, and combined lateral and torsional loading were used to verify the accuracy of the proposed approach.

2 Method of analysis

The problem of a pile group with arbitrarily distributed piles subjected to applied horizontal loads and torque is summarized in Fig. 1a. The rectangle represents the cap of the pile group and the circles represent the piles fixed to the cap. Define the coordinate X-Y with origin O as the global coordinate

system. (X_i, Y_i) indicates the coordinates of pile i, where i is from 1 to n. F_j is an applied horizontal load acting on the pile cap, where j is from 1 to m. F_{Xj} and F_{Yj} are the components of F_j in the X and Y directions, respectively. (X_{Fj}, Y_{Fj}) is the location of the action point of F_j. T is the applied torque on the pile cap. In this approach, the following assumptions are made: (1) the pile cap is rigid and not in contact with the ground; (2) the pile shafts are vertical, circular, elastic, and fixed to the pile cap, and obey the small deformation assumption; (3) each pile works as a simple beam and there is no separation between the soil and the pile; (4) the soil nonlinear response at the individual piles is modeled by load transfer curves (i.e. p-y and τ-θ curves); (5) the overturning angles of the pile cap (Fig. 1b) in two horizontal directions are small enough to be negligible, thus the motion of the pile cap is considered as a plane rigid-body motion.

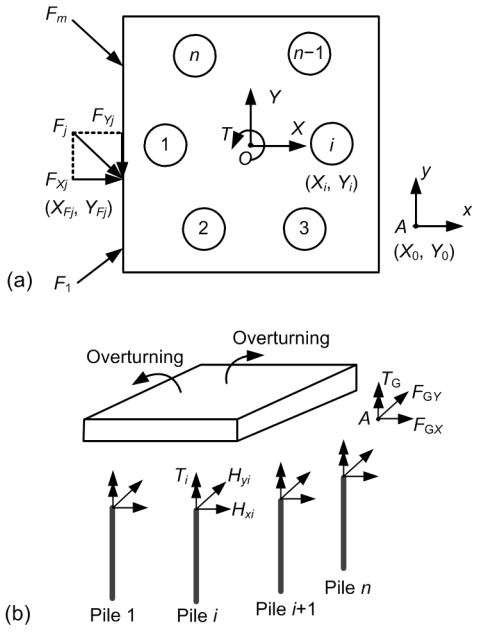

Fig. 1 An arbitrarily distributed pile group subjected to horizontal and torsional loads

(a) Top view; (b) 3D view. T_i, H_{xi}, H_{yi}, T_G, F_{GX}, and F_{GY} will be explained in the following text

2.1 Motions of piles in a pile group under combined lateral and torsional loading

Since the motion of the pile cap is considered as a plane rigid-body motion, a twist center exists at any time, called the instantaneous center, about which there is rotation without translation. It is assumed that point A in Fig. 1a is the instantaneous center of the pile cap and (X_0, Y_0) indicates its coordinates in the X-Y plane. The number of degrees of freedom for the plane motion of the pile cap is three: two coordinates being used to describe the translation and one to describe the rotation of the pile cap. In this study, X_0 and Y_0 are used to describe the translation of the cap, and φ to describe the pure rotation about point A. It is assumed that the instantaneous center of the pile cap is unchanged under a given applied load. Thus, the motion of the cap can be simplified as a pure rotation about point A. It is convenient to introduce a local coordinate system x-y with origin A in the current analysis (Fig. 1a). The local coordinates are fixed on the instantaneous center A and remain parallel to the global coordinates X-Y. Fig. 2a shows the motion of pile i in the pile group subjected to combined lateral and torsional loading in the local coordinates x-y. Pile i rotates from the initial position B through a rotation angle φ to the final position E. u_i and v_i are the components of the displacement of the pile head s_i in the x and y directions, respectively. θ_i is the angle from the x-axis to the line connecting the pile and the instantaneous twist center. d_i is the distance between pile i and the instantaneous center A. (X_i−X_0, Y_i−Y_0) indicates the coordinates of pile i in the local coordinate system. Referring to the geometric relationships in ΔABF and ΔAEG in Fig. 2a, the following equations apply:

$$d_i = \frac{X_i - X_0}{\cos\theta_i} = \frac{Y_i - Y_0}{\sin\theta_i}, \tag{2}$$

$$X_i - X_0 + u_i = d_i \cos(\theta_i + \varphi). \tag{3}$$

Substituting Eq. (2) into Eq. (3) yields the x-coordinate of pile i in the local coordinate system after the pile group is twisted:

$$X_i - X_0 + u_i = (X_i - X_0)\cos\varphi - (Y_i - Y_0)\sin\varphi. \tag{4}$$

Similarly,

$$Y_i - Y_0 + v_i = (Y_i - Y_0)\cos\varphi + (X_i - X_0)\sin\varphi. \tag{5}$$

From Eqs. (4) and (5), X_0 and Y_0 are expressed as

$$\begin{cases} X_0 = X_i + \dfrac{1}{2}\left(u_i - v_i \cot\dfrac{\varphi}{2}\right), \\ Y_0 = Y_i + \dfrac{1}{2}\left(v_i + u_i \cot\dfrac{\varphi}{2}\right). \end{cases} \tag{6}$$

Solving Eq. (6) yields

$$\begin{cases} u_i = -2\sin\dfrac{\varphi}{2}\left[(Y_i - Y_0)\cos\dfrac{\varphi}{2} + (X_i - X_0)\sin\dfrac{\varphi}{2}\right], \\ v_i = 2\sin\dfrac{\varphi}{2}\left[(X_i - X_0)\cos\dfrac{\varphi}{2} - (Y_i - Y_0)\sin\dfrac{\varphi}{2}\right]. \end{cases} \tag{7}$$

Since the pile cap is considered as a plane motion of a rigid body without overturning, u_i and v_i can be expressed by a given point in the plane in which the pile cap exists, which is defined as the reference point. Assume that the coordinates of the reference point are X_R and Y_R and its horizontal displacements are u_R and v_R. From Eq. (7), the relationship between the pile head displacements of pile i and the displacement of the reference point is expressed as

$$\begin{cases} u_i = \dfrac{(Y_i - Y_0)\cos\dfrac{\varphi}{2} + (X_i - X_0)\sin\dfrac{\varphi}{2}}{(Y_R - Y_0)\cos\dfrac{\varphi}{2} + (X_R - X_0)\sin\dfrac{\varphi}{2}} u_R, \\ v_i = \dfrac{(X_i - X_0)\cos\dfrac{\varphi}{2} - (Y_i - Y_0)\sin\dfrac{\varphi}{2}}{(X_R - X_0)\cos\dfrac{\varphi}{2} - (Y_R - Y_0)\sin\dfrac{\varphi}{2}} v_R. \end{cases} \tag{8}$$

From Eq. (8), both u_R and v_R remain non-zero and the coordinates of the reference point should satisfy $X_R \neq X_0$ and $Y_R \neq Y_0$. Since X_0 and Y_0 are unknown, it is proposed that a point near the equivalent action point of the resultant force of the applied lateral loads is used as the reference point. The equivalent loading position can be calculated by

$$\begin{cases} X_R = \dfrac{T_G F_{GY}}{F_{GX}^2 + F_{GY}^2}, \\ Y_R = -\dfrac{T_G F_{GX}}{F_{GX}^2 + F_{GY}^2}, \end{cases} \tag{9}$$

where $T_G = \sum_{j=1}^{m}(F_{Yj}X_{Fj} - F_{Xj}Y_{Fj}) + T$, $F_{GX} = \sum_{j=1}^{m} F_{Xj}$, and $F_{GY} = \sum_{j=1}^{m} F_{Yj}$. In practice, one of the pile centers close to the equivalent action point is preferred to minimize the calculation workload. As a special case, if $F_{GX}=F_{GY}=0$ and $T_G \neq 0$, the reference point is one of the corner pile centers in the group.

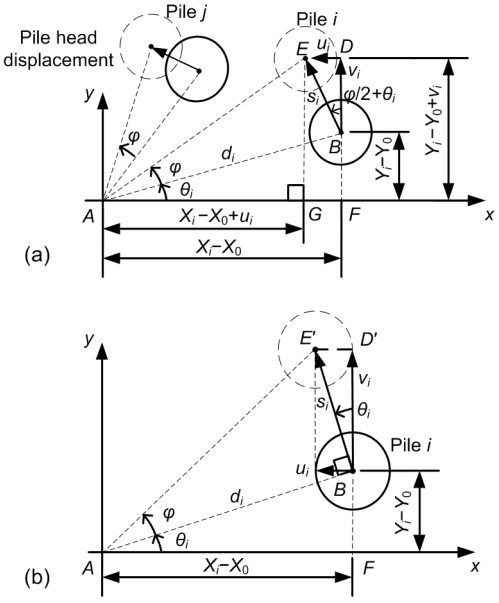

Fig. 2 Pile head horizontal displacements
(a) Exact version; (b) Simplified version

2.2 Static equilibrium equation of pile cap

Referring to Fig. 1b, which shows the pile cap subjected to external loads and internal forces on the pile heads, the equilibrium equations of the pile cap can be expressed as

$$\begin{cases} \sum_{i=1}^{n} H_{Xi} = F_{GX}, \\ \sum_{i=1}^{n} H_{Yi} = F_{GY}, \\ \sum_{i=1}^{n}[-H_{Xi}(Y_i - Y_0 + v_i) + H_{Yi}(X_i - X_0 + u_i) + T_i] \\ \quad = \sum_{j=1}^{m}[F_{Yj}(X_{Fj} - X_0) - F_{Xj}(Y_{Fj} - Y_0)] + T, \end{cases} \tag{10}$$

where H_{Xi} and H_{Yi} are the components of the pile head shear force on pile i in the x and y directions,

respectively, and T_i is the torque at the head of pile i. The relationships between the pile head forces and pile head displacements are expressed as

$$\begin{cases} H_{Xi} = K_{\mathrm{H}i} u_i, \\ H_{Yi} = K_{\mathrm{H}i} v_i, \\ T_i = K_{\mathrm{T}i} \varphi_i, \end{cases} \tag{11}$$

where $K_{\mathrm{H}i}$ and $K_{\mathrm{T}i}$ are the horizontal secant stiffness and torsional secant stiffness of pile i, respectively. Since the pile shaft is circular in cross section, the horizontal stiffness in the x and y directions are equal. Substituting Eqs. (4), (5), (8), and (11) into Eq. (10), the equilibrium equations of the cap can be further expressed as

$$\begin{cases} u_{\mathrm{R}} \sum\limits_{i=1}^{n} K_{\mathrm{H}i} \dfrac{(Y_i - Y_0)\cos\dfrac{\varphi}{2} + (X_i - X_0)\sin\dfrac{\varphi}{2}}{(Y_1 - Y_0)\cos\dfrac{\varphi}{2} + (X_1 - X_0)\sin\dfrac{\varphi}{2}} = F_{GX}, \\ v_{\mathrm{R}} \sum\limits_{i=1}^{n} K_{\mathrm{H}i} \dfrac{(X_i - X_0)\cos\dfrac{\varphi}{2} - (Y_i - Y_0)\sin\dfrac{\varphi}{2}}{(X_1 - X_0)\cos\dfrac{\varphi}{2} - (Y_1 - Y_0)\sin\dfrac{\varphi}{2}} = F_{GY}, \\ -u_{\mathrm{R}} \sum\limits_{i=1}^{n} K_{\mathrm{H}i} \dfrac{(Y_i - Y_0)\cos\dfrac{\varphi}{2} + (X_i - X_0)\sin\dfrac{\varphi}{2}}{(Y_1 - Y_0)\cos\dfrac{\varphi}{2} + (X_1 - X_0)\sin\dfrac{\varphi}{2}} \\ \quad \times \left[(Y_i - Y_0)\cos\varphi + (X_i - X_0)\sin\varphi\right] \\ \quad + v_{\mathrm{R}} \sum\limits_{i=1}^{n} K_{\mathrm{H}i} \dfrac{(X_i - X_0)\cos\dfrac{\varphi}{2} - (Y_i - Y_0)\sin\dfrac{\varphi}{2}}{(X_1 - X_0)\cos\dfrac{\varphi}{2} - (Y_1 - Y_0)\sin\dfrac{\varphi}{2}} \\ \quad \times \left[(X_i - X_0)\cos\varphi - (Y_i - Y_0)\sin\varphi\right] + \varphi \sum\limits_{i=1}^{n} K_{\mathrm{T}i} \\ \quad = \sum\limits_{j=1}^{m} [F_{Yj}(X_{Fj} - X_0) - F_{Xj}(Y_{Fj} - Y_0)] + T. \end{cases} \tag{12}$$

Eq. (12) is a coupled ternary transcendental equation and u_{R}, v_{R}, and φ can be solved using a binary algorithm. u_i and v_i, as well as s_i, can be further calculated from Eq. (8). Although an exact solution can be obtained from Eq. (12), the solving process is very time-consuming. However, Eq. (12) can be further simplified based on the assumption of small deformation, and an explicit solution in a simple form can be obtained. Based on the assumption of small deformation, the following approximations can be obtained:

$$\sin\frac{\varphi}{2} \doteq 0, \tag{13}$$

$$\sin\varphi \doteq \varphi, \tag{14}$$

$$\cos\varphi \doteq \cos\frac{\varphi}{2} \doteq 1. \tag{15}$$

Substituting Eqs. (13) and (15) into Eq. (8) yields

$$\begin{cases} u_i \doteq \dfrac{Y_i - Y_0}{X_0 - X_{\mathrm{R}}} v_{\mathrm{R}}, \\ v_i \doteq \dfrac{X_i - X_0}{X_{\mathrm{R}} - X_0} v_{\mathrm{R}}. \end{cases} \tag{16}$$

Fig. 2b shows the simplified geometric deformation of pile i. The direction of s_i is perpendicular to the line connecting the instantaneous center A and pile center B. In Fig. 2b, $\triangle ABF$ and $\triangle BE'D'$ are similar, and so

$$\frac{v_i}{X_i - X_0} = \frac{s_i}{d_i} \doteq \varphi. \tag{17}$$

Substituting Eqs. (13)–(17) into Eq. (12), the equilibrium equation can be simplified as

$$\begin{cases} \dfrac{v_{\mathrm{R}}}{X_0 - X_{\mathrm{R}}} \sum\limits_{i=1}^{n} K_{\mathrm{H}i}(Y_i - Y_0) = F_{GX}, \\ \dfrac{v_{\mathrm{R}}}{X_0 - X_{\mathrm{R}}} \sum\limits_{i=1}^{n} K_{\mathrm{H}i}(X_0 - X_i) = F_{GY}, \\ \dfrac{v_{\mathrm{R}}}{X_0 - X_{\mathrm{R}}} \sum\limits_{i=1}^{n} \{K_{\mathrm{H}i}[(X_0 - X_i)^2 + (Y_i - Y_0)^2] + K_{\mathrm{T}i}\} \\ \qquad = \sum\limits_{j=1}^{m} [F_{Yj}(X_{Fj} - X_0) - F_{Xj}(Y_{Fj} - Y_0)] + T. \end{cases} \tag{18}$$

Given $\sum\limits_{j=1}^{m} [F_{Yj}(X_{Fj} - X_0) - F_{Xj}(Y_{Fj} - Y_0)] + T \neq 0$, the solution of Eq. (18) is

$$\begin{cases} X_0 = \dfrac{b}{a} - \dfrac{F_{GY}(ag + ah + ad - b^2 - c^2)}{acF_{GX} - abF_{GY} + a^2 q - a^2 r + a^2 T}, \\ Y_0 = \dfrac{c}{a} + \dfrac{F_{GX}(ag + ah + ad - b^2 - c^2)}{acF_{GX} - abF_{GY} + a^2 q - a^2 r + a^2 T}, \\ v_{\mathrm{R}} = \dfrac{F_{GY}}{a} - \dfrac{(b - aX_{\mathrm{R}})(cF_{GX} - bF_{GY} + aq - ar + aT)}{a^2 g + a^2 h + a^2 d - ab^2 - ac^2}, \end{cases} \tag{19}$$

where $a=\sum_{i=1}^{n}K_{\mathrm{H}i}$, $b=\sum_{i=1}^{n}K_{\mathrm{H}i}X_i$, $c=\sum_{i=1}^{n}K_{\mathrm{H}i}Y_i$, $d=\sum_{i=1}^{n}K_{\mathrm{T}i}$, $g=\sum_{i=1}^{n}K_{\mathrm{H}i}X_i^2$, $h=\sum_{i=1}^{n}K_{\mathrm{H}i}Y_i^2$, $q=\sum_{j=1}^{n}F_{Yj}X_{Fj}$, and $r=\sum_{j=1}^{n}F_{Xj}Y_{Fji}$.

As $\sum_{j=1}^{m}[F_{Yj}(X_{Fj}-X_0)-F_{Xj}(Y_{Fj}-Y_0)]+T=0$, the pile group is actually subjected to lateral loading without torque, and the displacement for each pile is the same:

$$\begin{cases}u_i=\dfrac{F_{\mathrm{G}X}}{a},\\ v_i=\dfrac{F_{\mathrm{G}Y}}{a}.\end{cases}\tag{20}$$

In Eq. (19), the horizontal stiffness $K_{\mathrm{H}i}$ and the torsional stiffness $K_{\mathrm{T}i}$ for each pile in the pile group are affected by the way the pile head is restrained, pile shaft stiffness, free-standing length, soil stiffness, and pile-soil-pile interactions. In the present approach, the load transfer approach (i.e. *p*-*y* and *τ*-*θ* curves) is used to simulate the nonlinear springs representing the soil along the pile shaft. The generalized *p*-multiplier is adopted to consider the dominant part of the group effect in pile groups subjected to combined lateral and torsional loading. The coupling effect between lateral and torsional pile responses is also considered to modify the torsional stiffness.

3 Horizontal stiffness K_{H} and torsional stiffness K_{T}

An individual pile in the pile group shown in Fig. 1 is subjected to a lateral load, a bending moment, and a torsional load at the pile head. Assuming each pile works as a simple beam, the governing fourth- and second-order differential equations for the lateral deflection *s* and twist angle *φ* of the pile can be given by

$$E_{\mathrm{p}}I_{\mathrm{p}}\frac{\partial^4 s}{\partial z^4}+k_{\mathrm{h}}s=0,\tag{21}$$

$$G_{\mathrm{p}}J_{\mathrm{p}}\frac{\partial^2 \varphi}{\partial z^2}-k_{\tau}\varphi=0,\tag{22}$$

where $E_{\mathrm{p}}I_{\mathrm{p}}$ and $G_{\mathrm{p}}J_{\mathrm{p}}$ denote the bending stiffness and the torsional stiffness of the pile shaft, respectively; k_{h} and k_{τ} are the moduli of subgrade reaction for the grouped pile subjected to lateral loading and torsional loading, respectively. To consider the influence of the group effect on the pile, k_{h} is expressed as

$$k_{\mathrm{h}}=f_{\mathrm{m}}\frac{p}{s},\tag{23}$$

where f_{m} is the *p*-multiplier. To take account of the deflection-torsion coupling effect, k_{τ} is expressed as

$$k_{\tau}=\alpha_{\mathrm{TH}}\frac{\tau}{\theta},\tag{24}$$

where α_{TH} is called the torsional resistance amplification factor.

Each pile is modeled by a number of discrete beam elements (Fig. 3). The soil stiffness per unit length of a pile for lateral loading and for torsional loading are both represented by nonlinear springs at the nodal points of the elements. Based on the conventional finite element method (Smith et al., 2015), the force-deformation relationship of the pile may be written as

$$\boldsymbol{K}_{\mathrm{p}}\boldsymbol{w}_{\mathrm{p}}=\boldsymbol{Q}+\boldsymbol{P}_{\mathrm{p}},\tag{25}$$

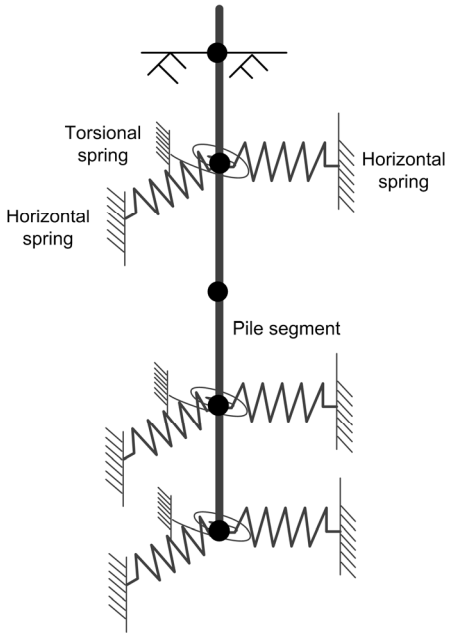

Fig. 3 Discrete elements of a pile

where $\boldsymbol{K}_\mathrm{p}$ is the global stiffness matrix of all elements of the pile; $\boldsymbol{w}_\mathrm{p}$ indicates the deformation of pile nodes; $\boldsymbol{Q}$ indicates external loads; $\boldsymbol{P}_\mathrm{p}$ indicates pile-soil interaction forces acting on the pile.

The load-displacement relationship for the soil at the nodes in the pile can be expressed by

$$\boldsymbol{P}_\mathrm{s} = \boldsymbol{K}_\mathrm{s}\boldsymbol{w}_\mathrm{s}, \tag{26}$$

where $\boldsymbol{P}_\mathrm{s}$ indicates the pile-soil interaction forces acting on the soil; $\boldsymbol{K}_\mathrm{s}$ is the soil stiffness matrix; $\boldsymbol{w}_\mathrm{s}$ indicates the soil displacement vector. The reaction moduli k_h and k_τ in $\boldsymbol{K}_\mathrm{s}$, which vary at different load levels, are evaluated using Eqs. (23) and (24), respectively. The p-y and τ-θ curves needed in Eqs. (23) and (24) are possibly from a field or model test on an instrumented pile. Alternatively, recommended p-y curves are usually used in practice (e.g. p-y curves for saturated sand are recommended by Reese et al. (1974)). f_m and α_TH will be proposed in the next two sections.

Based on the assumption of no separation between the soil and the pile, the compatibility of the deformations of the soil and the pile yields

$$\boldsymbol{w}_\mathrm{s} = \boldsymbol{w}_\mathrm{p}. \tag{27}$$

Equilibrium of the interaction forces acting at the pile-soil interface yields

$$\boldsymbol{P}_\mathrm{s} = -\boldsymbol{P}_\mathrm{p}. \tag{28}$$

Substituting Eqs. (26)–(28) into Eq. (25), the complete load-displacement relationship for the pile under lateral and torsional loading is given by

$$(\boldsymbol{K}_\mathrm{p} + \boldsymbol{K}_\mathrm{s})\boldsymbol{w}_\mathrm{p} = \boldsymbol{Q}. \tag{29}$$

The pile head is assumed fixed; therefore, the horizontal and torsional load-displacement relationships of the pile, K_H and K_T respectively, can be predicted by Eq. (29).

4 Generalized *p*-multiplier

The generalized p-multiplier of pile i in a pile group with n piles subjected to combined lateral and torsional loading is calculated using Eq. (1). To calculate β_{ji} in Eq. (1), the leading pile and the trailing pile are first defined according to Kong et al. (2019) to characterize the relative positions of pile i and pile j based on the horizontal motions of the two piles. Fig. 4 shows the movements of pile i and pile j in the horizontal plane. $\boldsymbol{s}_i$ and $\boldsymbol{s}_j$ are the displacements of pile i and pile j, respectively. Take the directions of both component vectors along the line connecting the two piles as a reference. If one of the two components along the connecting line is a non-zero vector and points to a pile, as shown in Fig. 4a, the pointed pile is called the leading pile, while the other pile is the trailing pile. Conversely, if the pile is located in the opposite direction to the non-zero component vector (Fig. 4b), it is the trailing pile, while the other pile is the leading pile. As a special case, if the components of both instantaneous velocities along the connecting line are zero vectors, the two piles can be designated arbitrarily. In Fig. 4, pile i is the leading pile, while pile j is the trailing pile. Kong et al. (2019) found that the angles between the directions of motion of the leading and trailing piles and the line through both piles, denoted by η and δ, vary in the ranges of 0°–90° and −90°–90°, respectively. Referring to the definitions of the leading pile and the trailing pile, the discriminant formula is

$$\boldsymbol{s}_i \cdot \boldsymbol{d}_{ji} = u_i(X_i - X_j) + v_i(Y_i - Y_j)$$
$$\begin{cases} >0, & \text{pile } i \text{ is the leading pile,} \\ <0, & \text{pile } i \text{ is the trailing pile,} \\ =0, & \text{further judgement based on pile } j, \end{cases} \tag{30}$$

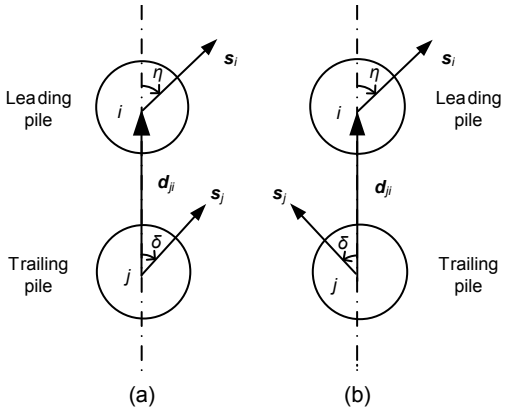

Fig. 4 Two motion states of a double-pile group subjected to combined lateral and torsional loading
(a) Two-pile motion on the same side; (b) Two-pile motion on different sides

where $\boldsymbol{s}_i=[u_i, v_i]^{\mathrm{T}}$ is the horizontal displacement vector of pile i, and $\boldsymbol{d}_{ji}=[X_i-X_j, Y_i-Y_j]^{\mathrm{T}}$ is the distance vector which points from pile j to pile i (Fig. 4). Further judgement in the third case uses the dot multiplication of $\boldsymbol{s}_j$ with $\boldsymbol{d}_{ji}$ as well. When both $\boldsymbol{s}_i\cdot\boldsymbol{d}_{ji}=0$ and $\boldsymbol{s}_j\cdot\boldsymbol{d}_{ji}=0$, either pile can be designated as the leading pile or the trailing pile.

Assume that pile i is the leading pile and pile j is the trailing pile in the double-pile group (Fig. 4). If the horizontal displacement vector of pile i, $\boldsymbol{s}_i$, is not zero, η is calculated by

$$\begin{aligned}\eta&=\arccos\frac{\boldsymbol{s}_i\cdot\boldsymbol{d}_{ji}}{|\boldsymbol{s}_i||\boldsymbol{d}_{ji}|}\\&=\arccos\frac{u_i(X_i-X_j)+v_i(Y_i-Y_j)}{\sqrt{u_i^2+v_i^2}\sqrt{(X_i-X_j)^2+(Y_i-Y_j)^2}}.\end{aligned}\tag{31}$$

If the displacement vector of pile j, $\boldsymbol{s}_j$, is not zero, then first it is necessary to determine whether δ is positive or negative. δ is positive when the displacement directions of the leading pile and the trailing pile are on the same side of the line connecting the two piles, and negative when they are on different sides. The proposed discriminant formula is

$$\begin{aligned}&(\boldsymbol{s}_j\times\boldsymbol{d}_{ji})\cdot(\boldsymbol{s}_i\times\boldsymbol{d}_{ji})\\&\quad=(\boldsymbol{s}_j\cdot\boldsymbol{s}_i)(\boldsymbol{d}_{ji}\cdot\boldsymbol{d}_{ji})-(\boldsymbol{d}_{ji}\cdot\boldsymbol{s}_i)(\boldsymbol{s}_j\cdot\boldsymbol{d}_{ji})\\&\quad\begin{cases}>0, & \text{same side},\\<0, & \text{different sides}.\end{cases}\end{aligned}\tag{32}$$

For the 'same side' case (Fig. 4a),

$$\begin{aligned}\delta&=\arccos\frac{\boldsymbol{s}_j\cdot\boldsymbol{d}_{ji}}{|\boldsymbol{s}_j||\boldsymbol{d}_{ji}|}\\&=\arccos\frac{u_j(X_i-X_j)+v_j(Y_i-Y_j)}{\sqrt{u_j^2+v_j^2}\sqrt{(X_i-X_j)^2+(Y_i-Y_j)^2}}.\end{aligned}\tag{33}$$

For the 'different sides' case (Fig. 4b),

$$\begin{aligned}\delta&=-\arccos\frac{\boldsymbol{s}_j\cdot\boldsymbol{d}_{ji}}{|\boldsymbol{s}_j||\boldsymbol{d}_{ji}|}\\&=-\arccos\frac{u_j(X_i-X_j)+v_j(Y_i-Y_j)}{\sqrt{u_j^2+v_j^2}\sqrt{(X_i-X_j)^2+(Y_i-Y_j)^2}}.\end{aligned}\tag{34}$$

If either $\boldsymbol{s}_i$ or $\boldsymbol{s}_j$ is zero, let $\eta=\delta=90°$ for convenience in calculation.

As η and δ are known, β_{ji} can be calculated using the empirical equations proposed by Kong et al. (2019), which are briefly summarized in Appendix A.

5 Deflection-torsion coupling effect

Kong and Zhang (2008b) and Kong et al. (2015) found that the torsional resistance of a pile subjected to combined lateral and torsional loading can be improved significantly by lateral loading, namely the deflection-torsion coupling effect. Kong and Zhang (2008b) discussed the mechanism of the coupling effect and proposed an amplification factor α_{TH} to quantify it:

$$\alpha_{\mathrm{TH}}=1+\frac{\beta_{\mathrm{TH}}}{p_{\mathrm{a}}D}p,\tag{35}$$

where β_{TH} is the deflection-torsion coupling factor (0.4 for loose sand and 0.8 for dense sand), p_{a} is standard atmospheric pressure, and D is the diameter of the pile.

6 Solution of the problem

A computer program, named ELPGROUP, was developed using this approach. A flow chart of the program is shown in Fig. 5. Input parameters include soil parameters, pile parameters, group configuration, and external loads. The loop operation of the p-multipliers starts with an initial value of 1. By calculating the horizontal stiffness and the torsional stiffness of each pile in a given pile group, the displacements of each pile are obtained through an internal iterative process. Then new p-multiplier of each pile is calculated using the newly-obtained displacements. The above process is repeated until p-multipliers satisfy a given tolerance. Note that the internal iterative process shown in Fig. 5 uses Eq. (19) (the solution of the simplified equilibrium equation). Therefore, the program has good efficiency in calculation, but obtains approximate results. To verify their accuracy, the approximate results were compared with model test results and exact solutions, as discussed in the next two sections.

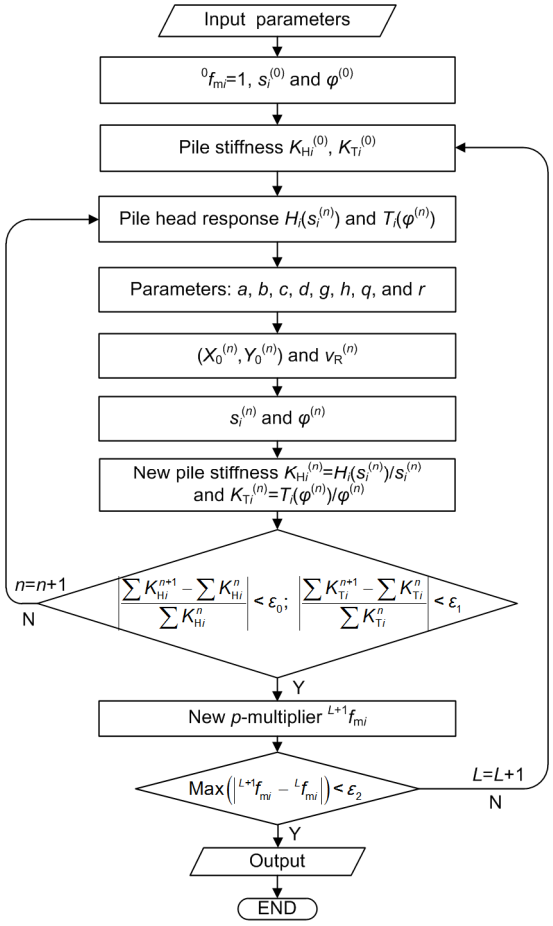

Fig. 5 Flow chart of ELPGROUP

ε_0, ε_1, and ε_2 are parameters for controlling accuracy; L is the number of cycles of the p-multipliers

7 Comparison with test results

The proposed approach is capable of simulating pile groups subjected to lateral loading, torsion, and combined lateral and torsional loading. Four model tests involving these three types of loading modes were adopted to verify the proposed approach.

7.1 Centrifuge model tests on horizontally loaded pile groups

Centrifuge tests of 3×3 pile groups at three-diameter (3D) and five-diameter (5D) spacings were carried out (McVay et al., 1995). The model piles simulated pipe piles 430 mm in diameter and 13.16 m long with a bending stiffness, EI, of 72.1 MN·m^2 embedded in medium loose (relative density D_r=33%) and medium dense (D_r=55%) sands. The embedded length of the piles in the prototype was 11.48 m. The p-y curves of sand proposed by Reese et al. (1974) were used to simulate the nonlinear response of the soil. For the medium loose sand, the angle of internal friction was 34°, Poisson's ratio was 0.3, the unit weight was 14.51 kN/m^3, and the modulus of subgrade reaction was selected as 8.14 MN/m^3. For the medium dense sand, the corresponding parameters were 39°, 0.3, 15.18 kN/m^3, and 24.4 MN/m^3, respectively. Figs. 6a and 6b show the load-displacement curves and the contributions of three different rows of a 3×3 pile group in medium dense sand and medium loose sand, respectively. In both figures, the predicted results from our proposed approach agree well with the reported experimental data.

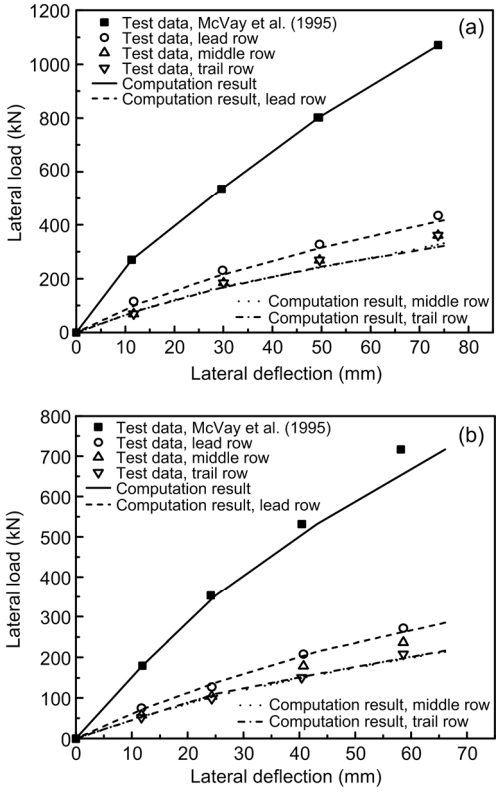

Fig. 6 Lateral load-displacement curves of a 3×3 pile group at 3D: (a) medium dense sand; (b) medium loose sand

7.2 Centrifuge model tests on torsionally loaded pile groups in sand

Results of centrifuge model tests conducted by Kong and Zhang (2007) on a torsionally loaded 3×3 pile group with a pile spacing of 3D in loose sand

were used to further verify the proposed approach. Aluminum model piles 19 mm in diameter and 300 mm in length were used in the centrifuge model tests to simulate a 3D spaced closed-end pipe pile group with a prototype outside diameter of 0.76 m, a pile length of 12.6 m, and an embedded length of 10.8 m. The bending stiffness of the piles was 220.5 MN·m^2, and Poisson's ratio was 0.3. The deflection-torsion coupling factor was 0.4. This simulation used the *p*-*y* and *τ*-*θ* curves of Kong and Zhang (2009). Fig. 7 shows the experimental torque-twist angle curve of the 3×3 pile group subjected to torsion, and the corresponding numerical predictions using the present model, and those of He et al. (2010) and Kong and Zhang (2009). The calculation curve obtained using the present approach fits the test data quite well and agrees well with that predicted by He et al. (2010).

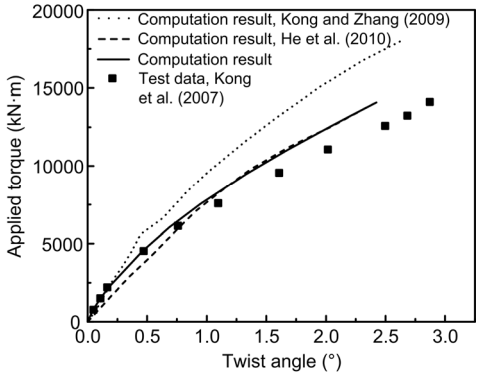

Fig. 7 Applied torque-twist angle curves of a 3×3 pile group in loose sand

7.3 Centrifuge test on a 2×2 pile group subjected to combined lateral and torsional loading

A centrifuge model test on a 2×2 pile group subjected to combined lateral and torsional loading were performed in sand at 80*g* (*g* is the acceleration of gravity) in this study to further verify the proposed approach. A hydraulic cylinder was used to apply a pulling force on the model pile cap. A load cell was assembled at the head of the hydraulic cylinder to measure the applied horizontal load. The system for measuring pile cap horizontal displacements consisted of four Wenglor laser-displacement sensors: two along the actuator and two in the perpendicular direction. The measurements from any three laser-displacement sensors can be used to calculate the twist angle of the pile cap and the two horizontal displacements at the center of the pile cap (Kong and Zhang, 2007). The instrumented model piles were manufactured using a 500 mm-long aluminum tube, with an outside diameter of 16 mm and a wall thickness of 1.5 mm. Different types of strain gauges were installed on the external surface of the four piles to measure the bending moment, shear force, axial force, and torque on the pile heads. To protect the strain gauges, the whole pile surface was coated with epoxy resin and the pile diameter was increased to 20 mm. The pile cap for the 2×2 pile group, prefabricated using aluminum plates, was 100 mm wide and 30 mm thick. The model test was conducted at 80*g*. Thus, the model piles simulated 3D spaced closed-end pipe pile groups with a prototype outside diameter of 1.6 m, a total length of 40 m, and an embedded length of 35.6 m. The flexural stiffness of the piles was 5.12 GN·m^2, Poisson's ratio 0.3, and the torsional rigidity of the piles 3.94 GPa.

Fujian standard sand was used in this study. This sand is uniform quartz sand with a specific gravity of 2.63. The mean diameter is 0.17. The uniformity coefficient, C_u, was 1.58. The maximum and minimum unit weights were 16.06 kN/m^3 and 13.22 kN/m^3, respectively, and the corresponding minimum and maximum void ratios were 0.61 and 0.95, respectively (Kong et al., 2019). The unit weights and relative densities of the sand used in the tests were 15.18 kN/m^3 and 62.9%, respectively.

Two single pile tests, a torsional pile test and a lateral pile test, were conducted in the same soil bed to obtain *p*-*y* curves and *τ*-*θ* curves, which were used to simulate the 2×2 pile group tests. Ten levels of bending moment strain gauges were installed on the external surface of the laterally loaded single pile to measure the distribution of bending moments on the model pile. The approach proposed by Kong and Zhang (2007) was used to derive experimental *p*-*y* curves. The curve-fitting equation of the experimental *p*-*y* curves was

$$p=\frac{a(z)y}{b(z)+y}, \tag{36}$$

where $a(z)$ and $b(z)$ are the functions of depth z, obtained by curve fitting. In the torsionally loaded single pile test, a torsional cylinder was used to load the model pile at the pile head. Nine levels of torsional

strain gauges were also installed on the external surface of the model pile to measure the distribution of torsional force along the pile shaft. The approach proposed by Kong (2006) was used to derive experimental τ-θ curves. The curved fitted result was

$$\tau = \frac{A(z)B(z)\theta}{A(z)\theta + B(z)}, \tag{37}$$

where $A(z)$ and $B(z)$ were obtained by curve fitting.

The p-y and τ-θ curves originating from the tests were input into ELPGROUP to simulate the responses of the laterally and torsionally loaded single piles. The test data were compared with the computation results of the laterally loaded pile test (Fig. 8a) and the torsionally loaded pile test (Fig. 8b). The computation results agree well with the test data. Fig. 9 shows the pile cap response of the pile group under combined lateral and torsional loading. Fig. 10 further shows the pile head horizontal displacements of the group piles. In both figures, the results predicted by the proposed approach agree well with the test data.

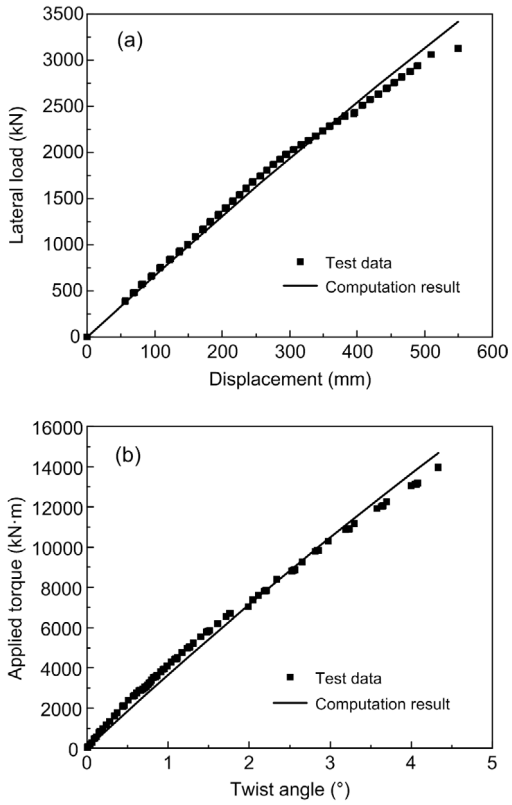

Fig. 8 Comparison of experimental and computation results of single piles: (a) laterally loaded single pile test; (b) torsionally loaded single pile test

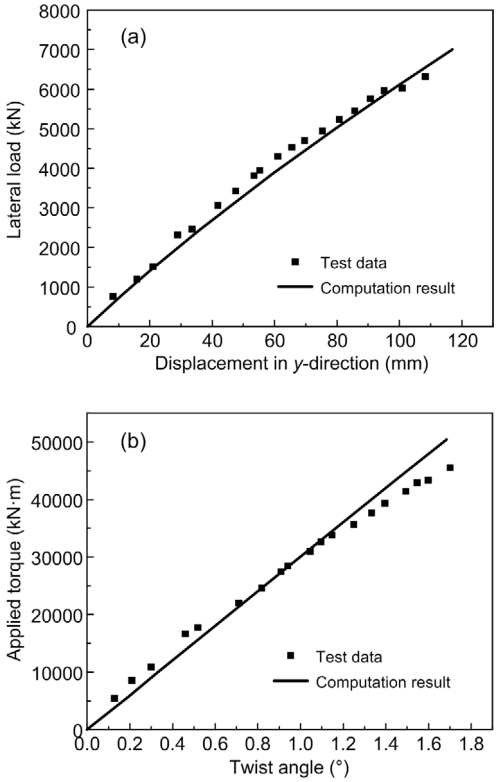

Fig. 9 Response of a 2×2 pile group subjected to combined lateral and torsional loading: (a) lateral load-horizontal displacement curve; (b) applied torque-twist angle curve

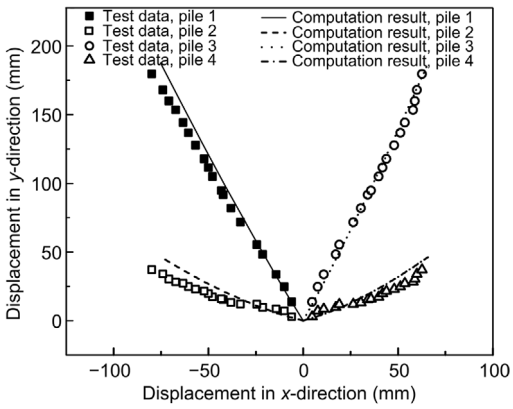

Fig. 10 Pile head displacements of individual piles in a 2×2 pile group subjected to combined lateral and torsional loading

7.4 Large model test on a 3×3 pile group subjected to combined lateral and torsional loading

Kong et al. (2015) reported a 3×3 pile group test in saturated silt laterally loaded at an eccentric distance of 6D. The model piles used were closed-end steel tubes with a diameter of 0.114 m, length of

5.95 m, embedded length of 3.41 m, and thickness of 4.5 mm. The soil used in the test was saturated silt. The *p*-*y* curves proposed by Reese et al. (1974) were adopted in this calculation. The input parameters were: modulus of subgrade reaction 23.464 MN/m^3, internal friction angle 30°, Poisson's ratio 0.2, and unit weight 8.8 kN/m^3. The τ-θ curves in the calculation were obtained from the formula proposed by Kong and Zhang (2009). The parameters in the formula (A=4.5×10^7 N/m^2, B=8800×0.23z N/m^2, A_t=1090 N/m, and B_t=52 N/m) were obtained by fitting data from a single pile torsional test.

Fig. 11 shows the experimental load-displacement curve and experimental torque-twist angle curve of the pile cap at a load eccentricity of 6D, and the corresponding numerical predictions using the present approach. There is good agreement at higher loading stages, whereas the analysis under-predicts the pile resistance at the initial loading stages. One of the reasons behind this under-prediction may be that the reduction factors predicted from the proposed empirical equations, as well as the calculated *p*-multipliers, tend to overestimate the interaction among piles with small pile displacements (Kong et al., 2019).

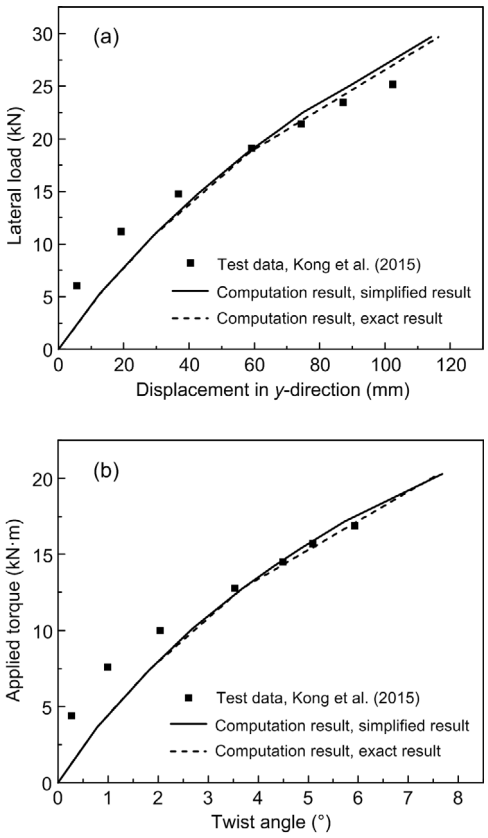

Fig. 11 Response of a 3×3 pile group subjected to combined lateral and torsional loading in saturated silt (Kong et al., 2015): (a) applied load-horizontal displacement curves of pile cap; (b) applied torque-twist angle curves of pile cap

8 Comparison between exact and approximate results

Fig. 11 also compares the approximate results with the exact results obtained by substituting the solutions of Eq. (12) into the internal iterative process. Fig. 12 shows the variation of the errors of the pile cap twist angle and pile head displacements with the pile cap twist angle. Piles 1, 2, and 3, which belong to three rows respectively, were chosen to show the errors of pile head displacements. The errors change with pile position. When the pile cap twist angle is small enough, the errors of the pile head displacements are negligible in application. For instance, when the pile cap twist angle is 5°, the maximum error of pile head displacements is only 4.8% (Pile 3). Therefore, the simplified solution developed by the present approach shows good accuracy in predicting the response of pile groups under combined lateral and torsional loading in small twists. To increase accuracy at large twist angles, Eqs. (6) and (8) can be adopted to calculate the pile head displacements of individual piles after X_0, Y_0, and v_R are obtained from the simplified solution.

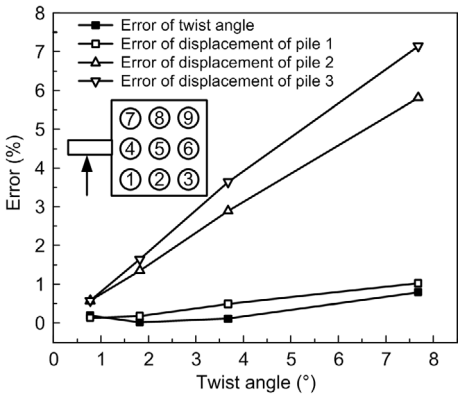

Fig. 12 Errors of the pile cap twist angle and pile head displacements

9 Conclusions

In this study, a simple and computationally efficient approach has been developed for analyzing the nonlinear response of pile groups under combined lateral and torsional loading. Previous studies showed that the pile cap motion of a pile group subjected to combined lateral and torsional loading is a combination of horizontal and torsional movements, and can be seen as a plane rigid-body motion. An explicit pile head displacement relationship of the grouped piles and static equilibrium equations of the pile cap were derived according to the concept of instantaneous center in a plane rigid-body motion. The generalized p-multiplier proposed by Kong et al. (2019) is used in this approach to account for the horizontal interaction among the individual piles, which has a dominant effect on the response of the pile groups. The coupling effect of the lateral resistance and torsional resistance of each pile was quantified using an empirical factor β. The lateral and torsional nonlinear responses of individual piles were modeled using p-y and τ-θ curves. Since the p-multipliers for individual piles vary with the direction of motion of the piles, an iteration scheme was developed to calculate the p-multiplier values and the pile head displacements of the piles. An approximate equilibrium equation of the pile cap was derived to improve the computational efficiency in iteration.

Model tests on pile groups subjected to lateral loading, torsional loading, and combined lateral and torsional loading, separately, were predicted using the proposed approach. In general, the pile cap response and the transfer of applied loads in the pile groups were predicted with good accuracy.

Contributors

Ling-gang KONG designed the research. Ling-gang KONG and Zhong-chang ZHANG processed the corresponding data. Zhong-chang ZHANG wrote the first draft of the manuscript. Ling-gang KONG and Yun-min CHEN revised and edited the final version.

Conflict of interest

Ling-gang KONG, Zhong-chang ZHANG, and Yun-min CHEN declare that they have no conflict of interest.

References

Brown DA, Morrison C, Reese LC, 1988. Lateral load behavior of pile group in sand. *Journal of Geotechnical Engineering*, 114(11):1261-1276. https://doi.org/10.1061/(asce)0733-9410(1988)114:11(1261)

Chen SL, Kong LG, Zhang LM, 2016. Analysis of pile groups subjected to torsional loading. *Computers and Geotechnics*, 71:115-123. https://doi.org/10.1016/j.compgeo.2015.09.004

Gu M, Kong LG, Chen RP, et al., 2014. Response of 1×2 pile group under eccentric lateral loading. *Computers and Geotechnics*, 57:114-121. https://doi.org/10.1016/j.compgeo.2014.01.007

He W, Chen RP, Kong LG, et al., 2010. Bearing behaviors and nonlinear theory of pile groups subjected to torque. *Chinese Journal of Geotechnical Engineering*, 32(5):751-756 (in Chinese).

Hu ZH, McVay M, Bloomquist D, et al., 2006. Influence of torque on lateral capacity of drilled shafts in sands. *Journal of Geotechnical and Geoenvironmental Engineering*, 132(4):456-464. https://doi.org/10.1061/(asce)1090-0241(2006)132:4(456)

Kong LG, 2006. Behaviour of Pile Groups Subjected to Torsion. PhD Thesis, The Hong Kong University of Science and Technology, Hong Kong, China. https://doi.org/10.14711/thesis-b924406

Kong LG, Zhang LM, 2007. Centrifuge modeling of torsionally loaded pile groups. *Journal of Geotechnical and Geoenvironmental Engineering*, 133(11):1374-1384. https://doi.org/10.1061/(asce)1090-0241(2007)133:11(1374)

Kong LG, Zhang LM, 2008a. Effect of pile-cap connection on behavior of torsionally loaded pile groups. *Journal of Zhejiang University-SCIENCE A*, 9(3):303-312. https://doi.org/10.1631/jzus.a0720022

Kong LG, Zhang LM, 2008b. Experimental study of interaction and coupling effects in pile groups subjected to torsion. *Canadian Geotechnical Journal*, 45(7):1006-1017. https://doi.org/10.1139/t08-038

Kong LG, Zhang LM, 2009. Nonlinear analysis of torsionally loaded pile groups. *Soils and Foundations*, 49(2):275-286. https://doi.org/10.3208/sandf.49.275

Kong LG, Chen RP, Wang SH, et al., 2015. Response of 3×3 pile groups in silt subjected to eccentric lateral loading. *Journal of Geotechnical and Geoenvironmental Engineering*, 141(7):04015029. https://doi.org/10.1061/(asce)gt.1943-5606.0001313

Kong LG, Fan JY, Liu JW, et al., 2019. Group effect in piles under eccentric lateral loading in sand. *Journal of Zhejiang University-SCIENCE A (Applied Physics & Engineering)*, 20(4):243-257. https://doi.org/10.1631/jzus.a1800617

Li Q, Stuedlein AW, 2018. Simulation of torsionally loaded deep foundations considering state-dependent load transfer. *Journal of Geotechnical and Geoenvironmental Engineering*, 144(8): 04018053. https://doi.org/10.1061/(asce)gt.1943-5606.0001930

Li Q, Stuedlein AW, Barbosa AR, 2019. Role of torsional shear in combined loading of drilled shaft foundations. *Journal*

of Geotechnical and Geoenvironmental Engineering, 145(4):06019001. https://doi.org/10.1061/(asce)gt.1943-5606.0002039

Li ZF, 2015. Response and Effect Factors of Pile Groups Subjected to Eccentric Lateral Loading. MS Thesis, Zhejiang University, Hangzhou, China (in Chinese).

McVay M, Casper R, Shang TI, 1995. Lateral response of three-row groups in loose to dense sands at 3D and 5D pile spacing. *Journal of Geotechnical Engineering*, 121(5):436-441. https://doi.org/10.1061/(asce)0733-9410(1995)121:5(436)

Mehra S, Trivedi A, 2018. Experimental studies on model single pile and pile groups subjected to torque. *In*: Wu W, Yu HS (Eds.), Proceedings of China-Europe Conference on Geotechnical Engineering. Springer, Cham, Switzerland, p.997-1000. https://doi.org/10.1007/978-3-319-97115-5_24

Randolph MF, 1980. PIGLET: a Computer Program for the Analysis and Design of Pile Groups under General Loading Conditions. Soil Report TR91, University of Cambridge, Cambridge, UK.

Reese LC, Cox WR, Koop FD, 1974. Analysis of laterally loaded piles in sand. Proceedings of the 6th Annual Offshore Technology Conference, p.473-485. https://doi.org/10.4043/2080-ms

Reese LC, Wang ST, Vasquez L, 2006. Computer Program GROUP 7.0—Technical Manual. Ensoft, Inc., Austin, USA.

Smith IM, Griffiths DV, Margetts L, 2015. Programming the Finite Element Method, 5th Edition. John Wiley & Sons, Chichester, UK.

Xu KJ, Poulos HG, 2000. General elastic analysis of piles and pile groups. *International Journal for Numerical and Analytical Methods in Geomechanics*, 24(15):1109-1138. https://doi.org/10.1002/1096-9853(20001225)24:15<1109::AID-NAG72>3.0.CO;2-N

Xue J, Gavin K, Murphy G, et al., 2016. Optimization technique to determine the *p-y* curves of laterally loaded stiff piles in dense sand. *Geotechnical Testing Journal*, 39(5):842-854. https://doi.org/10.1520/gtj20140257

Appendix A

Reduction factors of the leading pile and trailing pile, β_l and β_t, can be calculated using a series of elliptic formulas if η, δ, and the pile spacing are known:

$$\beta_l=\begin{cases} b_l-\dfrac{b_l-a_l}{|\delta_c|}\sqrt{\delta_c^2-\delta^2}, \\ \qquad\qquad 0>\delta\geq\delta_c, \text{ or } \delta_c\geq\delta\geq 0, \\ 1, \quad 0>\delta_c\geq\delta\geq -90^\circ, \text{ or } 90^\circ\geq\delta\geq\delta_c>0, \end{cases} \tag{A1}$$

$$\beta_t=\begin{cases} b_t-\dfrac{b_t-a_t}{|\delta_c|}\sqrt{\delta_c^2-\delta^2}, \\ \qquad\qquad 0>\delta\geq\delta_c, \text{ or } \delta_c\geq\delta\geq 0, \\ 1, \quad 0>\delta_c\geq\delta\geq -90^\circ, \text{ or } 90^\circ\geq\delta\geq\delta_c>0, \end{cases} \tag{A2}$$

where a_l and a_t are reduction factors β_l and β_t, respectively, for the case that δ=0° at some given value of η, while b_l and b_t are reduction factors β_l and β_t, respectively, for the case that $\delta=\delta_c$. δ_c is a reference parameter. $\delta_c=\delta_0$ with the existence of the critical angle, otherwise δ_c=90° when $\delta\in$[0°, 90°], or δ_c=−90° when $\delta\in$[−90°, 0°).

a_l and a_t, as well as b_l and b_t, are not consistent with varying η. Kong et al. (2019) proposed quadratic parabolic functions to calculate a_l and a_t, and piecewise functions to calculate b_l and b_t.

中文概要

题　目： 水平偏心受荷群桩的非线性分析

目　的： 群桩基础在近海建/构筑物及桥梁中广泛应用，而风、浪、船舶撞击等在群桩基础中产生的水平和扭转荷载往往影响群桩基础的安全。本文旨在提出一套能够计算水平和扭转荷载联合作用下的群桩非线性响应简化分析方法。

创新点： 1. 采用广义 *p* 乘子法考虑群桩中各桩水平变形导致的桩−土−桩相互作用；2. 建立基于瞬时转动中心的基桩桩头位移关系和承台平衡方程。

方　法： 1. 通过理论分析给出基桩桩头位移之间的关系，建立承台平衡方程；2. 采用荷载传递模型（*p-y* 和 *τ-θ* 曲线）模拟桩周土体非线性响应；3. 采用广义 *p* 乘子法考虑群桩中各桩水平变形导致的桩−土−桩相互作用，并采用耦合因子计算基桩中推−扭耦合响应；4. 通过迭代方法求解各基桩 *p* 乘子和群桩响应。

结　论： 1. 多组算例均表明本文提出的群桩非线性分析模拟能够较准确地模拟群桩响应，尤其在承台位移较大的情况下；2. 广义 *p* 乘子能够有效地模拟群桩效应的主要部分；3. 模型中的简化公式能够应用于实际工程问题分析。

关键词： 水平和扭转组合荷载；群桩；转动中心；*p* 乘子；群桩效应